Modelling Computed Radiography Detectors with a Cascaded Linear System Model

Françoise MATHY*, Andreas SCHUMM**, Joachim TABARY*, Patrick HUGONNARD*
*LETI-Minatec Campus – CEA Grenoble– 38054 Grenoble – Cedex 9 France
**EDF-R&D SINETICS Clamart France
Contact: francoise.mathy@cea.fr

Abstract. Computed radiography systems consist of an assembly of an imaging plate, an optical reading system, and an acquisition system [1,2]. In the imaging plate, the incoming radiation is first absorbed in a sensitive layer and subsequently converted to optical photons. Then the latent image is read through an optical system and converted into an electrical signal, and eventually into grey values. Standards [3,4] for these systems were published in 2005.
To model them in a realistic way, a cascaded linear system model developed in SINDBAD [5] is proposed. In this model, the user builds its own detector by cumulating several linear processes such as amplification process, blurring and noise process for each physical phenomenon involved in the detection.
If used with a high energy source, the signal is reinforced with a metallic screen. This effect has also to be taken into account to optimize the right exposure conditions for a given problem and to get the right signal to noise ratio (SNR). Preliminary simulations with PENELOPE [6], a Monte Carlo code, are compared with the analytical approach implemented in SINDBAD.

Introduction

The use of storage phosphor Image Plates (IP or PSP) instead of film systems in Computed Radiography for NDT has increased during last years as specific devices have been developed by manufacturers. Standards [3-4] for classification of systems and principles of testing metallic materials with these systems were published in 2005.
Several radiographic chain simulators have been developed since the 90s. They include models for several kinds of detectors, such as standard pixelated detectors, film systems, flat panels (see a recent review [7]). The aim of this paper is to present the first steps for the design of a model of CR detectors through already existing modalities.

1. The basic processes of CR: a multistep process

1.1 The physics of CR

The reader can refer to recent review papers in medical field [1,2].
Fig. 1 [2] summarizes the steps of formation of the image in Image Plates (IP) or PhotoStimulable Phosphor plates (PSP):
(1) Image acquisition involves exposing the patient (object) with a study-specific x-ray technique and recording the transmitted x-ray flux with the PSP detector.

(2) The resultant latent image is extracted via the reader device using laser stimulation and recording the PSL intensity.
(3) Image pre-processing involves correcting systematic variations in the extraction process and determining the range of pertinent information with subsequent adjustment of digital values to a normalized output range.
(4) Image post-processing translates the digital values of the raw digital image to render a greyscale and frequency enhancement appropriate for the detail investigated.
(5) The output image is displayed on a calibrated image monitor for presentation.

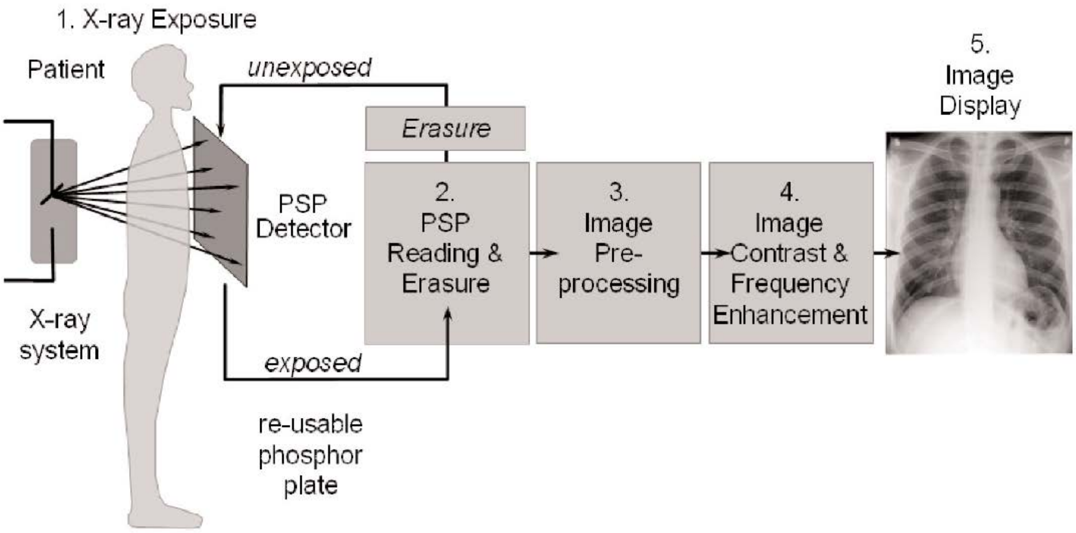

Figure 1. PSP Image acquisition and processing can be divided into five separate steps [2].

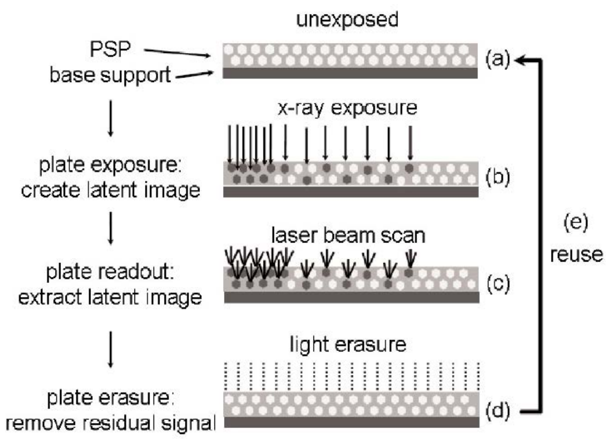

Figure 2. The phosphor plate cycle [2]

The phosphor plate cycle is outlined in fig. 2.
(a) An unexposed plate comprises the PSP material layered on a base support and protected by a thin, transparent coating.
(b) Exposure to x-rays creates latent image centres of electrons metastable energy traps in the crystal structure.
(c) Latent image processing is accomplished with a raster-scanned laser beam. Trapped electrons are released from the luminescent centres and produce light that is collected by a light guide assembly and directed to a PMT.
(d) Residual trapped electrons are removed with a high-intensity light source, and
(e) The plate is returned to the cassette for reuse.

The PSP material consists of a mixture of small grains of BaFX:Eu^{2+} in a binder (made of organic material). It is deposited on a polymer substrate, usually Mylar. Between the substrate layer and the sensitive layer, there is a light absorbing or reflective layer (for sensitivity or resolution optimization). The PSP material is protected by a thin layer. The packing factor of the sensitive layer is ~60%. One can see the stack in fig. 3 [8], as well as typical PSP material thicknesses. The binder can include an organic dye to absorb the stimulating laser light for spatial resolution optimisation.

The manufacturers [9-12] propose high resolution IPs HR (40-50 mg/cm^2) and HS (70-100 mg/cm^2) ones. Each type of screen uses a different grain size. The screen thickness should not be larger than 10-20 times grain size for light diffusion considerations, hence spatial resolution.

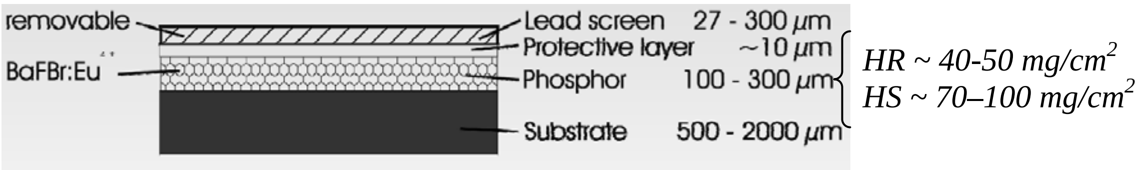

Figure 3. Structure of the PSP layer [8].

Table 1 [1] summarizes the main properties of the different PSP powder materials.

Table 1. Physical properties of the main powder photostimulable components [1]. G is the conversion gain (emitted light photons per 50 keV of absorbed energy when fully stimulated).

Photostimulable Phosphor	Z	Ek (keV) K-edge	Density (g/cm3)	G (phot /50keV)	Decay time (µs)	Light emission peak (nm)	Spectrum for stimulation (nm)
BaFBr:Eu^{2+}	56	37.4	5.1	140	0.7	390	500-650
$BaFBr_{0.85}I_{0.15}$:Eu^{2+}	56/53	37.4/33.2	(2.1)	140	0.7	390	550-700
BaFI:Eu^{2+}	56/53	37.4/33.2	(~5.6)		0.6	405	550-700

The scanning of the plate is done usually with a flying laser spot. This should not degrade the intrinsic spatial resolution performance, if correctly designed and used. (For instance, degradation can come from excessive laser spot power).

1.2 Performances

The light emitted is proportional to the energy absorbed in the sensitive layer for over four decades.

Due to the light diffusion in the sensitive layer, absorption or reflection of emitted light, the spatial resolution is not as good as for films. It is described through the Modulation Transfer Function (MTF). See [1-2, 9-13].

The performance of the whole system, which is a combination of sensitivity, spatial resolution and noise, can be described through its Detection Quantum Efficiency (DQE)

$$DQE= (SNR_{out}^2 / SNR_{in}^2).$$

The decomposition of the DQE can be made into a few steps [2] or more detailed [1].

At last, there is a saturation of SNR with dose, due to IP structural noise [1,8].

1.3 High energy specificity

As for film systems, one uses metallic screens in front and back of the image plate to enhance the signal through secondary X photons and electrons produced inside the screens, and to filter the low energy scattered signal. (see the recommendations in [4]).

2. The cascade model

2.1 State of the art

The succession of different linear stages leads to the use of a cascade model. This type of model was introduced by Cunningham & al [14]. The general idea is that a system is a succession of stages, and for each stage, mean signal and noise of the image are propagated according to typical formulae which depend on the kind of the process. The parameters are the global MTF (Modulation Transfer Function), the NPS (Noise Power Spectrum) and the DQE (Detective Quantum Efficiency).
A recent publication [16,17] shows a quite detailed cascade model for IP for medical applications. It does not include any screen, and requires a lot of physical parameters.
The cascade model developed in SINDBAD and used to simulate a flat panel [5] is a pragmatic model inspired by some Cunningham team works [15]. It carries signals and noise through different kinds of processes (amplification process, stochastic blurring process, deterministic blurring process, noise addition process). See on fig. 3 and table 2 the details of the process.

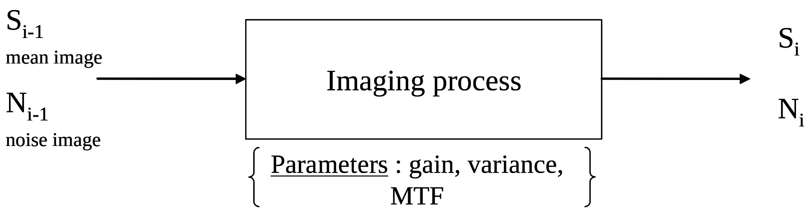

Figure 4. Input/output principle of linear imaging processes

Table 2. List of the elementary processes of a cascade model

	signal	noise
Amplification process	$S_i = g \times S_{i-1}$	N_i = Gaussian noise (mean = $g \times N_i$, variance = $N_{i-1} . \sigma^2_g$).
Deterministic spreading process	$S_i = S_{i-1}$ o PSF	$N_i = N_{i-1}$ o PSF
Stochastic spreading process	≡ Deterministic spreading process if enough quanta	
Noise addition process	$S_i = S_{i-1}$	N_i = Gaussian noise (mean = N_i, variance = σ^2_g)
Non linear conversion process	Conversion table	Conversion table

2.2 Proposed CR cascade model

We propose a simplified model using the different stages of the SINDBAD cascade model in Table 2. Some stages could be further split into substeps, if detail parameters can be found.
Considering the specific application for high energy, the first step of the model – energy absorption in the sensitive layer with or with no screen - is quite vital. It defines the sensitivity, hence hopefully the main component of the noise, quantum noise, if not in structural noise saturation zone. So to get a good SNR estimation we first focus on this step.

Table 3. Proposed cascade model for a CR system

Filtering by optional metallic screen	1: Beer-Lambert Attenuation 2: + MCarlo (if screen in object) secondary photon emission
Absorption in sensitive layer	Standard (+ quantum noise)
X-ray matter interaction blurring	Deterministic Spreading
Conversion to light through laser stimulation	Amplification (2.8 ph/keV) + noise
Light spread (in sensitive layer) + escape on reflective or absorbent layer*	spreading (MTF) Swank + stochastic amplification
Conversion to electrical signal (PMT)	amplification
Conversion to digital signal	Non-linear conversion
LUT application	Non-linear conversion
Electronics noise	noise

*The light spread and escape step can be split into more detailed processes (amplification). The structural noise of the IP should be added in this stage.

3. First steps of the cascade model: an evaluation with PENELOPE [6]

Using an Iridium 192 source to examine thick steel objects (see fig. 5), which is useful to get enough signal, generates much scattering which carries little useful information on small details. As the sensitive layer of the IP is quite sensitive to low energy (because of Barium), and not that much to high energy, it is recommended to put metallic screens (typically lead) in front and behind the IP, as for film systems. (see [4]). They enhance the signal through secondary photons and electrons emitted in the screens and filter the low energy scattered flux.

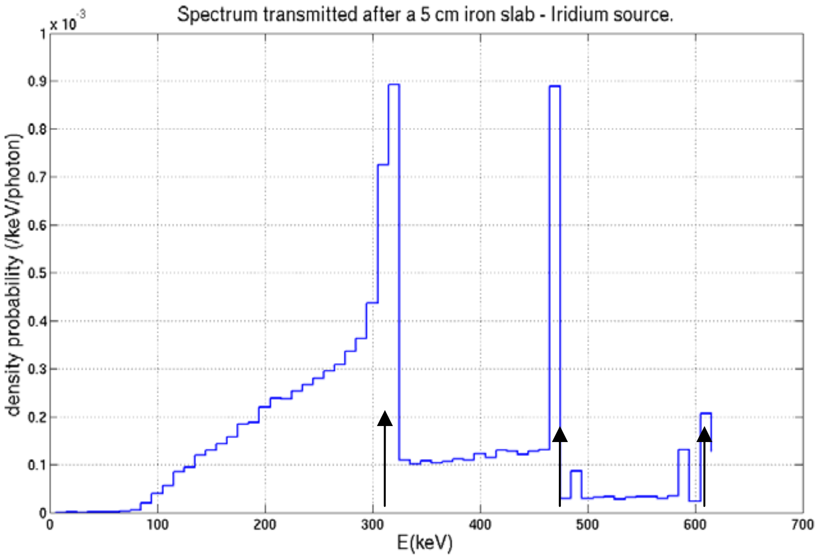

Figure 5. Spectrum transmitted after a 5 cm Fe slab. Iridium 192 source. (Arrows: the mains lines of an Iridium source).

The resultant light signal is proportional to the energy absorbed in the sensitive layer.
(G ~140 photons / 50 keV). See table 1.
In SINDBAD, there are two ways to take the screen into account:

1- The screen is a filter : Beer-Lambert attenuation in the filter, then absorption in the sensitive layer (thickness d) using the energy absorption factor

$\exp(-\mu_{tot\_screeb}*d_{screen}) * \mu_{ae}/\mu_{tot}*(1-\exp(-\mu_{tot}*d))$

2- The screen can be part of the object to be inspected, so that secondary photons can be generated in the screen as well as attenuation (Monte Carlo simulation)

We check with a full Monte Carlo code, PENELOPE, if the 1^{st} option is realistic.
The conditions of the simulation are: BaFBr HR 150 µm (packing factor 60%), Mylar-like protective layer 30 µm, and Mylar substrate under the BaFBr layer (300 µm).
3 setups:

- no screen
- 300 µm Pb front screen, 150 µm back screen
- 400 µm Pb front screen, 400 µm back screen (see EN 14784-2 [4])

Irradiation by monoenergetic pencil beam in cylindrical geometry.

Fig. 6 and 7 show the same results with different units. Fig. 6 shows the fraction of energy absorbed in the sensitive layer as a function of the photon energy. Fig. 7 shows the absorbed energy (keV) per g/cm^2 sensitive material. The last one is similar to the curve computed with MCNP for BaFBr alone in [18].
The use of Pb screens flattens the response quite efficiently, apart in the 70-80 keV area where there are the Pb K-edge and Pb fluorescence lines.
For both figures, there is the comparison between PENELOPE results and analytical formulae used in SINDBAD. For BaFBr alone, the discrepancy is significant over 200 keV. With Pb screens, the discrepancy begins at lower energies.
Clearly, it is not possible to simulate the Pb screen only as a filter for ^{192}Ir energies.
Further analysis will show whether as for films, one can also use the energy absorbed in the screen to give a better approximation of the IP response. Or if the secondary photon production is the essential contribution of the signal enhancement, as the protecting layer and substrate may absorb the secondary electrons partially. In this case, we can consider the screen as part of the object and compute secondary photon emission in it.

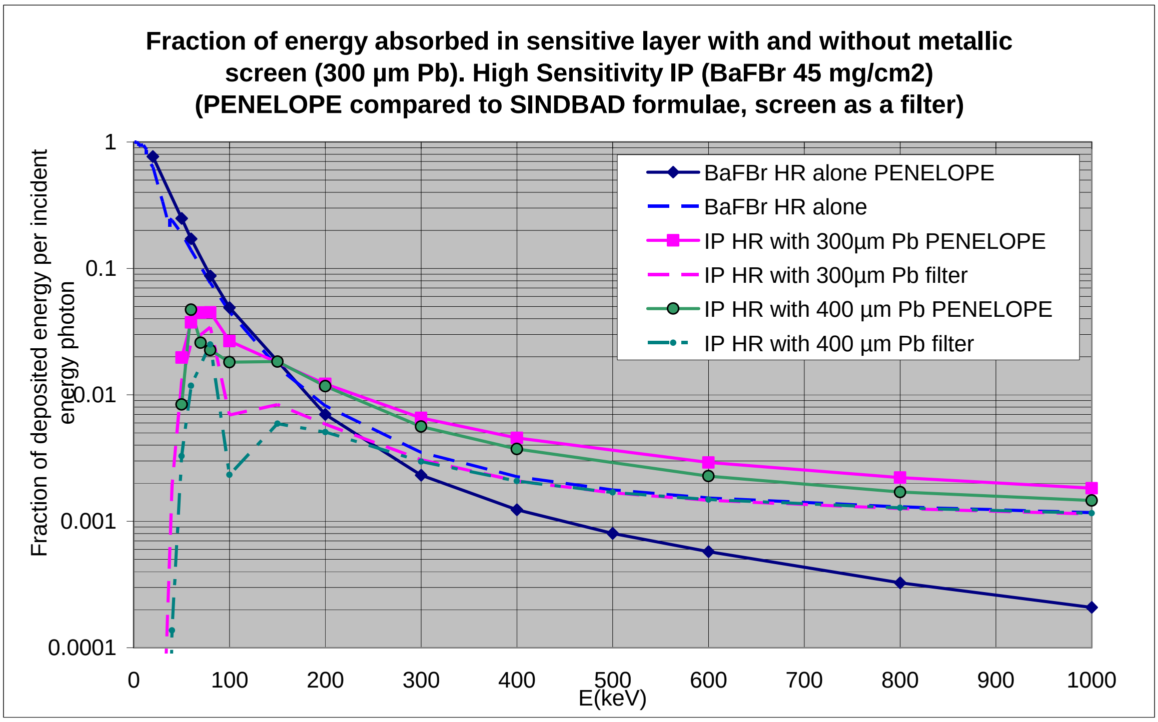

Figure 6. Fraction of absorbed energy of the incident photon in the sensitive layer (for an HR IP) with or without Pb screens

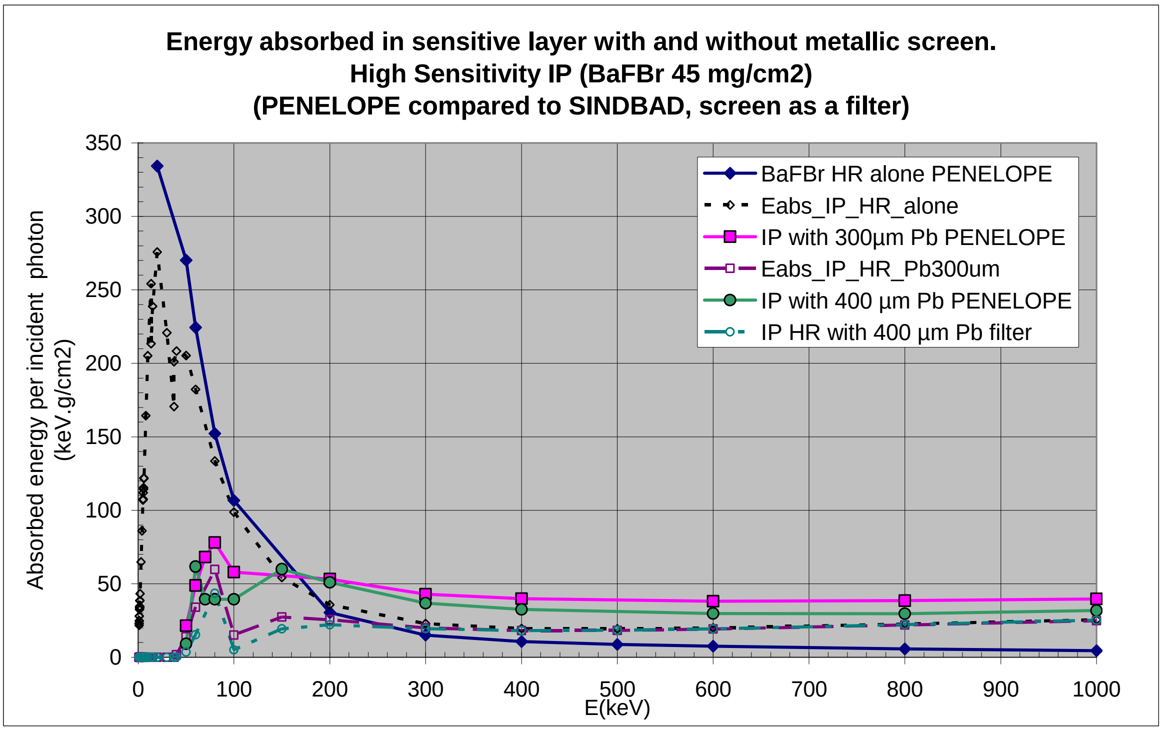

Figure 7. Energy absorbed in the sensitive layer (for an HR IP) with or without Pb screens as a function of incident photon energy (same as fig. 4)

Fig. 8 shows the energy spectrum of the signal absorbed in the sensitive layer for a 300 keV pencil beam. The Pb screen shifts the IP response towards higher energy. But the BaFBr layer is quite sensitive to the fluorescence Pb lines, which is not good for spatial resolution. The use of iron-like, copper or nickel sheets between BaFBr and Pb certainly attenuates these lines.

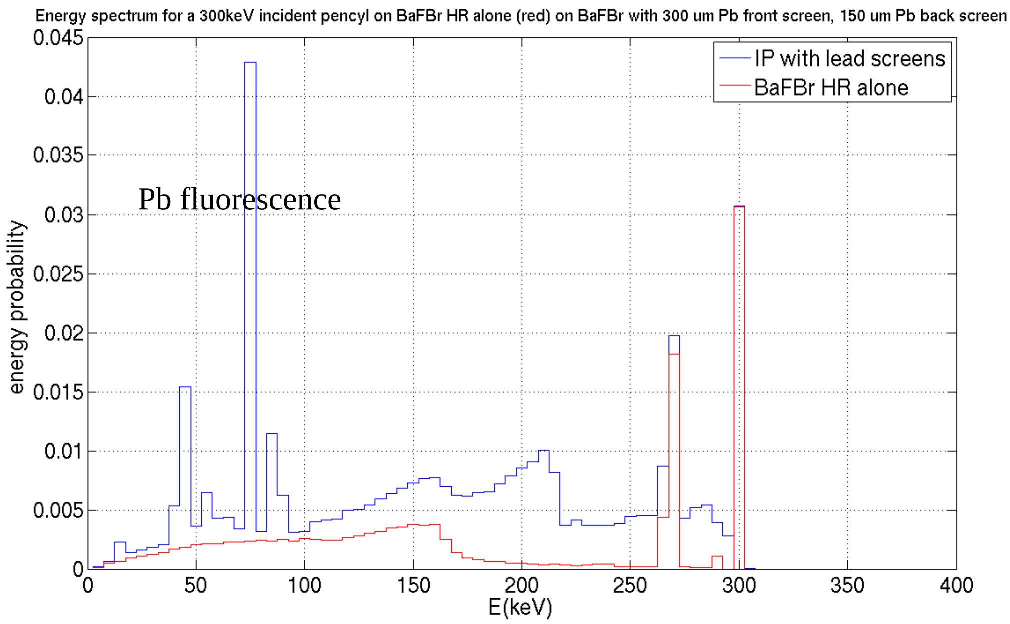

Figure 8. Absorbed spectra in the sensitive layer with lead screens (300 µm front/ 150 µm back, blue) and with no screen (red) for a 300 keV incident photon pencil beam.

Conclusion and perspectives

First steps for the development of a model for CR have been realized. To take into account the high energy NDT specificity, two ways are being investigated in parallel:
- use of the SINDBAD cascade model with as little steps as possible (search for synthetic performances)
- search for the 1st step (absorbed energy) reliable model - energy absorbed in the sensitive layer of an IP-screens system - with the help of a full Monte Carlo code, PENELOPE. This is the condition necessary to get a good SNR estimation.

The sensitivity response of a generic High Resolution Image Plate model to monoenergetic X-Ray photons up to 1 MeV has been simulated. Spatial resolution and response with more complex screens are under investigation.

More detailed information on specific CR systems is required to get a reliable model.

References

[1] J.A. Rowlands "The Physics of Computed Radiography" Phys. Med. Biol. 47 (2002) R123–R166
[2] AAPM Report no. 93, "Acceptance Testing and Quality Control of Photo Stimulable Phosphor Imaging Systems". Report of Task Group #10 American Association of Physicists in Medicine, octobre 2006
[3] EN 14784-1 "Non-destructive testing - Industrial computed radiography with storage phosphor imaging plates - Part 1: Classification of systems"
[4] EN 14784-2 "Non-destructive testing - Industrial computed radiography with storage phosphor imaging plates - Part 2: General principles for testing of metallic materials using X-rays and gamma rays"
[5] J. Tabary, P. Hugonnard, F. Mathy, "SINDBAD : a realistic multi-purpose and scalable X-ray simulation tool for NDT applications", Int. Symp. on DIR and CT, Lyon, June 2007.
[6] http://www.oecd-nea.org/science/pubs/2009/nea6416-penelope.pdf
[7] A. Schumm, P. Duvauchelle, V. Kaftandjian, R. Jaenisch, C. Bellon, J. Tabary, F. Mathy, S. Legoupil, "Modelling of radiographic inspections", NDTMS 2011 May 15-18, Istanbul.
[8] U. Zscherpel, U. Ewert,- (BAM) „Computed Radiography", Kalpakkam, India, 2007
[9] http://www.fujifilm.com/products/ndt/
[10] (http://www.ge-mcs.com/en/radiography-x-ray/digital-x-ray/phosphor-imaging-plates.html)
[11] http://www.carestreamhealth.com/nondestructivetesting.html
[12] CARESTREAM INDUSTREX : "Digital Imaging Plates Technical datasheet" February 2011 • TI-2632
[13] www.duerr-ndt.de
[14] http://www.imaging.robarts.ca/~icunning/html/publications.php
[15] J.P.Bissonnette, I.A.Cunningham, P.Munro : "Optimal phosphor thickness for portal imaging", Med. Phys. 24 (6), pp 803-813, 1997.
[16] Srinivasan Vedantham, and Andrew Karellas, "Modeling the Performance Characteristics of Computed Radiography (CR) Systems", IEEE TRANSACTIONS ON MEDICAL IMAGING, VOL. 29, NO. 3, march 2010
[17] Mike Sattarivand and I. A. Cunningham, "Computational Engine for Development of Complex Cascaded Models of Signal and Noise in X-Ray Imaging Systems", IEEE Transactions On Medical Imaging, Vol. 24, No. 2, February 2005
[18] S.C.A.Correa, & al, "Computed radiography simulation using the Monte Carlo code MCNPX", Appl Radiat Isot. 2010 Sep;68(9):1662-70.